Applied Catalysis B: Environmental 237 (2018) 116–127

Contents lists available at ScienceDirect

Applied Catalysis B: Environmental

journal homepage: www.elsevier.com/locate/apcatb

The influence of phosphorus on the catalytic properties, durability, sulfur resistance and kinetics of Cu-SSZ-13 for NO_x reduction by NH_3-SCR

Zhen Chen[a,1], Chi Fan[a,1], Lei Pang[b], Shujun Ming[a], Peng Liu[a], Tao Li[a,*]

[a] Key Laboratory of Material Chemistry for Energy Conversion and Storage, Ministry of Education, Hubei Key Laboratory of Material Chemistry and Service Failure, School of Chemistry and Chemical Engineering, Huazhong University of Science and Technology, Wuhan 430074, PR China
[b] DongFeng Trucks R&D Center, Zhushanhu Road No. 653, Wuhan 430056, PR China

ARTICLE INFO

Keywords:
NH_3-SCR
Cu-SSZ-13
Phosphorus poisoning
Durability
Sulfur poisoning resistance

ABSTRACT

The influence of phosphorus on the catalytic properties, durability, sulfur resistance and kinetics of Cu-SSZ-13 for NO_x reduction by ammonia selective catalytic reduction (NH_3-SCR) were systematically investigated to obtain a deeper understanding of the deactivation of Cu-SSZ-13 in the presence of phosphorus-containing impurities in diesel exhaust. An enhanced effect on NO conversion at low phosphorus loading was found above 450 °C, probably due to the reduction of copper oxides that promote NH_3 oxidation at high temperatures. As the phosphorus loading reached 0.4 mmol/g_{catal}, the framework dealumination and decrease of the BET specific surface area, acidity, and isolated Cu^{2+} ions accounted for the decrease in activity and hydrothermal stability over the entire temperature range. Simultaneously, the activity of phosphorus-impregnated samples tested in the presence of SO_2 indicates that phosphorus accelerates the deactivation of Cu-SSZ-13 in the presence of SO_2 at low temperatures, primarily due to the severe decrease of the Cu^{2+} ion content and partial coverage of the acid sites and active sites by phosphate and sulfate species. Additionally, kinetic analysis further demonstrated that phosphorus has an inhibitory effect on the SCR reaction rates at low temperatures and high phosphorus addition changes the NH_3-SCR reaction kinetic parameters. The data presented herein provide a comprehensive picture of the interaction between phosphorus and Cu-SSZ-13.

1. Introduction

Currently, ammonia selective catalytic reduction (NH_3-SCR) of NO_x has been proven to be the most economical and efficient technique for the removal of NO_x from diesel engine exhaust [1–3]. The discovery of Cu-CHabazite (Cu-CHA, including Cu-SSZ-13 and Cu-SAPO-34) catalysts has greatly advanced the commercialization of urea-SCR (the urea hydrolysis product, NH_3, is the actual reductant) technology to meet the present and emerging NO_x regulations due to their wide operating temperature window, low NH_3 slip, and significantly enhanced hydrothermal stability over other metal-exchanged zeolites (such as MFI and BEA zeolites) [4–7]. The copper-promoted SSZ-13 is preferred and has been commercialized for removing NO_x by urea-SCR from diesel engine exhaust [8–10]. Despite its successful application, Cu-SSZ-13 catalyst still faces numerous challenges concerning stability during the operating period.

Catalyst durability is a particularly important issue for automotive applications with increasingly stringent legal and practical application requirements [11]. The hydrothermal stability and the tolerance against chemical poisoning of the SCR catalyst are the most important issues [12–14]. The high-temperature exposure (> 650 °C) with the presence of moisture in the feed can damage the zeolite framework structure and lead to catalyst deactivation [14,15]. Therefore, resistance to hydrothermal aging can be crucial for NH_3-SCR catalyst applications. In addition, chemical poisoning originating from oil and fuel-derived contaminants can result in strong chemisorption of poisons on the active sites of a catalyst and a loss of specific surface area due to pore blocking [11,16,17]. Thus, high tolerance against catalyst poisons such as potassium, calcium, magnesium, sulfur, phosphorous and hydrocarbons is also highly desired [13,18]. Our recent works [19,20] have sufficiently studied the alkali and alkaline earth resistance and hydrothermal stability of Cu-SSZ-13 catalyst with different Si/Al ratios. It clearly clarified the deactivation mechanisms of steam and alkali poisoning on Cu-SSZ-13 and the catalyst with Si/Al = 15 showed excellent hydrothermal stability and alkali resistant ability.

Indeed, effects induced by another chemical poison, phosphorous, are also a major problem in practical applications of SCR catalysts due to their permanent deactivation by phosphorous-containing impurities

* Corresponding author.
E-mail address: taoli@hust.edu.cn (T. Li).
[1] These authors contributed equally to this work.

https://doi.org/10.1016/j.apcatb.2018.05.075
Received 6 February 2018; Received in revised form 24 May 2018; Accepted 26 May 2018
Available online 28 May 2018

in biodiesel and lubricant oil additives [1,21]. Several studies focused on the effect of phosphorous deactivation on oxide-based NH_3-SCR catalysts (V_2O_5-WO_3/TiO_2, CeO_2-MoO_3/TiO_2, Mn/TiO_2) [18,22,23] and Cu/Fe modified zeolites (BEA, ZSM-5) [1,13,24]. It was shown that phosphorous can greatly weaken the effectiveness of the NO_x emission control systems due to its cumulative influence over catalysts, which leads to a loss of specific surface area, pore blocking, disruption of the zeolite framework and a decrease of active sites. Weckhuysen et al. [25] also reviewed phosphorus–zeolite chemistry and revealed the universal physicochemical and structural effects of phosphorus–zeolite chemistry on the framework structure, accessibility, acid strength, catalytic performance and hydrothermal stability of H-ZSM-5. It clarifies that phosphorus can partially dislodge tetrahedrally coordinated framework aluminium species in ZSM-5, leading to a decrease in specific surface area and micropore volume, acid content and strength. However, to our best knowledge, only two studies are available that focus on the chemical deactivation of Cu-SSZ-13 caused by phosphorus [11,26]. Recently, Olsson et al. [26] examined the influence of phosphorus on Cu-SSZ-13 for various catalytic reactions, including standard SCR, NO oxidation and NH_3 oxidation. Interestingly, it was found that the effect of phosphorus on NO reduction was nearly negligible below 300 ℃ and a promotive effect was found above 300 ℃ due to severely suppressed ammonia oxidation and NO oxidation. However, a completely suppressing effect of phosphorus on the NH_3-SCR catalytic activity of Cu-SSZ-13 was found by Beale et al [11]. It indicates that the deactivation mechanisms of phosphorous on Cu-SSZ-13 are not completely understood. More importantly, the previous works are concentrated on the effect of phosphorous on physicochemical properties, catalytic activity and relevant side reactions over Cu-SSZ-13 catalyst. Nevertheless, the effect of phosphorous on the durability, sulfur poisoning resistance and NH_3-SCR reaction kinetics of Cu-SSZ-13 catalyst, which are the crucial factors for SCR catalyst in practical application, has gone virtually unreported in the open literature.

Hence, in this work, Cu-SSZ-13 catalyst was treated with various concentrations of $(NH_4)_2HPO_4$ aqueous solutions by a conventional impregnation method. The influence of phosphorus on the physicochemical properties (including zeolitic framework, acidity and copper species), catalytic activity, durability and sulfur poisoning resistance of Cu-SSZ-13 were evaluated by a series of characterization techniques including N_2 sorption, XRD, NMR, NH_3-TPD, H_2-TPR, EPR and catalytic reaction. In addition, NH_3-SCR kinetic tests were performed to explore the influence of phosphorus on the NH_3-SCR reaction chemistry of Cu-SSZ-13 catalyst.

2. Experimental

2.1. Sample preparation

2.1.1. Catalyst synthesis

The Cu-SSZ-13 catalyst (Si/Al = 15; 2.3 wt.% Cu) was synthesized via a hydrothermal method and then an ion-exchange process. The SSZ-13 was synthesized using a procedure similar to that reported previously [27,28]. The composition of the initial gel is as follows: 10 TMAda:10 NaOH:3.3 Al_2O_3:100SiO_2:2200 H_2O. The synthetic procedure and reagent quantities used are provided in the Supporting information. The Cu-SSZ-13 catalyst was prepared from SSZ-13 via an ion-exchange process as described elsewhere [29,30], and the detailed steps are provided in the Supporting information. The as-prepared Cu-SSZ-13 catalyst was notated Cu-F.

2.1.2. Phosphorus poisoning

The deactivation study of the calcined Cu-SSZ-13 powder was performed using aqueous $(NH_4)_2HPO_4$ solution as a phosphorus precursor by a conventional impregnation method [11,26]. To mimic practical conditions of diesel engine after-treatment system [11,26,31], three theoretical phosphorus poisoning levels were investigated: 0.1, 0.2 and 0.4 mmol g^{-1}, respectively. After impregnation, the samples were dried in an oven at 60℃ for 2 h and then at 110℃ for 12 h. The impregnated samples were calcined in air at 600℃ for 5 h at a ramp rate of 2℃·min^{-1}. The phosphorus-impregnated Cu-SSZ-13 was notated according to the deactivated level as Cu-0.1P, Cu-0.2P and Cu-0.4P, respectively.

2.1.3. Monolith catalyst preparation

The monolith catalyst was prepared as follows: certain amounts of water were added to the as-prepared powders and then were mixed to form well-proportioned slurries. A cordierite (cylinder, diameter: 11 mm, length: 22 mm, bulk: 2.1 cm^3, 400 cell cm^{-2}) was coated by dipping it into the slurries. The monolith catalyst was dried at 110℃ for 2 h and then weighed after each immersion. Successive immersions (approximately 3-4 times) of the cordierite in the suspension were performed to achieve the expected loading of approximately 250 g L^{-1}. Finally, approximately 300 mg of powder was washcoated to each cordierite.

2.1.4. Hydrothermal aging treatment after phosphorus poisoning

To investigate the effect of phosphorus on the durability of Cu-SSZ-13 catalyst, the as-prepared monolithic SCR catalyst was conducted with an accelerated hydrothermal aging process in a quartz tube reactor, containing 10% H_2O and 90% air flowing at the rate of 2000 cm^3 min^{-1} at 750 ℃ for 12 h. The hydrothermally aged sample of the Cu-SSZ-13 was named Cu-A. The hydrothermally aged sample after phosphorus poisoning according to the deactivated level was named Cu-0.1P-A, Cu-0.2P-A and Cu-0.4P-A, respectively.

2.1.5. Sulfur poisoning treatment after phosphorus poisoning

To investigate the effect of phosphorus on the sulfur poisoning resistance of Cu-SSZ-13 catalyst, the as-prepared monolithic SCR catalyst was evaluated with a typical reactant gas composition in the presence of SO_2: 1000 ppm NO, 1100 ppm NH_3, 5% O_2, 25 ppm SO_2, 10% H_2O and balance N_2. After activity evaluation, the monolithic catalyst was regenerated for characterization (except for N_2 sorption) after post-treatment in air at 550℃ for 2 h. The sulfurized sample of Cu-SSZ-13 was named Cu-S. The sulfurized sample after phosphorus poisoning according to the deactivated level was named Cu-0.1P-S, Cu-0.2P-S and Cu-0.4P-S, respectively.

2.2. Catalyst characterization

Prior to the characterization of aged and sulfurized samples, washcoat catalysts were carefully scraped from the monolith cores. The content of Si, Al, P and Cu was analyzed using ICP-AES (prodigy 7, Teledyne Leeman labs), after solid dissolution in HNO_3/HCl/HF aqueous solution. The BET specific surface area and micropore volume of the prepared catalysts were measured using BET specific surface area and micropore volume analyzer V-Sorb 2800 P. Before analysis, the samples were degassed at 250℃ for 5 h under vacuum (10^{-5} bar). Powder X-ray diffraction (XRD) patterns were recorded on an X'Pert Pro X-ray diffractometer over a 2θ range of $5^\circ - 40^\circ$ with the step size of 0.01° using Cu Kα irradiation. Solid–state ^{27}Al MAS NMR spectra were collected on an Agilent 600 MHz solid state NMR spectrometer operating at the spectral frequency of 79.52 MHz (Si). A relaxation delay of 10 s for Si was applied to collect single pulse spectra. All measurements were performed at room temperature, and $AlCl_3$ was used as an external reference. The temperature-programed desorption of ammonia (NH_3-TPD) was conducted on a Micromeritics AutoChem 2920 II instrument. The sample (0.05 g) was loaded into a U-shaped quartz tube and pretreated at 550℃ in an argon flow for 2 h. Then, the sample was cooled to 100℃ and saturated with NH_3 gas for 45 min. The sample was flushed with argon for 45 min to remove the physically adsorbed NH_3. The TPD profile of ammonia was obtained at a ramping rate of 10℃/min. The H_2-TPR experiments were also performed on a Micromeritics

AutoChem 2920 chemisorption analyzer. The sample (0.05 g) was placed in a quartz reactor and pretreated at 550℃ in a flow of argon (25 mL/min) for 2 h, and then cooled to room temperature. Then, H_2-TPR was performed in a 10 vol.% H_2/Ar gas flow of 10 ml/min at a heating rate of 10℃/min. UV-Vis-DRS spectra were obtained using a Shimadzu UV-3600 spectrometer equipped with an integrating sphere with $BaSO_4$ as the reference. The electron paramagnetic resonance (EPR) spectra were recorded on a JEOL-FA200 spectrometer to examine the structure and coordination of isolated Cu^{2+} ions. Powder samples (9.6 mg) were calcined at 600℃ for 6 h and then stored in 4 mm OD quartz tubes. All EPR spectra of Cu-SSZ-13 catalysts were also obtained at 115 K. The EPR measurement conditions were: modulation frequency 100 kHz, modulation amplitude 0.08 m T, scanning field 315.7 m T, sweep time 2 min, microwave power 0.998 mW, and microwave frequency 9.09 GHz.

2.3. NH_3-SCR catalytic activity test

The activity of the monolithic SCR catalyst was measured in a fixed-bed (VDRT-200SCR, Quzhou Vodo instrument Co. Ltd., China) with a stainless steel tubular reactor of 1.2 cm in diameter and 80 cm in length. The temperature was varied from 175 to 575℃, as measured using a type K thermocouple (in a stainless steel sheath) inserted directly into the center of the monolithic catalyst. The reactant gas composition was typical: 1000 ppm NO, 1100 ppm NH_3, 5% O_2, 10% water vapor and balance N_2. The water vapor was generated by passing de-ionized water through a preheating furnace and heating band (150 ℃) from a syringe pump (TYD01-01, LEAD FLUID). Under typical conditions, a 2.1 cm^3 monolithic catalyst was used in each test. The total flow rate was 1050 $cm^3\,min^{-1}$ and thus a GHSV by volume of 30,000 h^{-1} was obtained. The concentration of NO after the reaction was monitored using an exhaust analyzer (FGA-4100-5G, Foshan Analytical Instrument Co. Ltd.). To avoid errors caused by the oxidation of NH_3, an NH_3 trap containing phosphoric acid solution was installed before the gas entered the exhaust analyzer. The NO conversion was calculated from the following equation:

$$\text{NO conversion } (\%) = \frac{NO_{inlet} - NO_{outlet}}{NO_{inlet}} \times 100\ (\%)$$

2.4. The kinetic measurements

The NH_3-SCR kinetic tests were performed in a stainless steel tubular reactor. The loading of sample on cordierite was reduced from 250 g L^{-1} to 60 g L^{-1} to ensure the elimination of internal and external diffusion. The inlets consisted of 1000 ppm NO, 1100 ppm NH_3, 5% O_2 (25 ppm SO_2 when used) and, 10% H_2O with N_2 as the balance. The total flow rate was 1050 $cm^3{\cdot}min^{-1}$ and thus a GHSV by volume of 30,000 h^{-1} was obtained. The kinetic steady-state measurements were obtained in the temperature range of 100– 300 ℃. By assuming the reaction adheres to the plug flow reactor model and is free of diffusion limitations, the NH_3-SCR reaction rates can be calculated from the NO conversion as:

$$\text{rate } [\text{mol NO } g_{catal}\,s^{-1}] = -\frac{F_{NO}\ [L_{(NO)}\,min^{-1}] * \ln(1 - X_{NO}[\%])}{m_{catal}[g] * 60\ [s\,min^{-1}] * 22.4\ [L\,mol^{-1}]}\ [\text{mol NO } g_{catal}\,s^{-1}]$$

Here, X_{NO} is the conversion of NO, F_{NO} is the volumetric flow rate of NO, and m_{catal} is the mass of powder catalyst.

Table 1
Elemental analysis, specific surface area (S_{BET}) and total pore volume (V_{pore}) for NO_{inlet} the fresh and phosphorus-impregnated Cu-SSZ-13.

Sample	Cu loading (wt.%)	Theoretical P (wt.%)	Measured P (wt.%)	S_{BET} ($m^2\,g^{-1}$)	V_{pore} ($cm^3\,g^{-1}$)
Cu-F	2.3	0	0	622	0.216
Cu-0.1 P	2.3	0.31	0.24	608	0.212
Cu-0.2 P	2.4	0.62	0.56	596	0.207
Cu-0.4 P	2.4	1.24	1.22	561	0.189

3. Results and discussion

3.1. Effect of phosphorus on the physicochemical properties of Cu-SSZ-13

3.1.1. Compositions and structural properties

The chemical compositions of the fresh and phosphorus-impregnated Cu-SSZ-13 catalysts analyzed using ICP-AES are presented in Table 1. As expected, the fresh and phosphorus-impregnated Cu-SSZ-13 catalysts contain a similar copper content of approximately 2.3 wt.%. The measured content of phosphorous in Cu-0.1P, Cu-0.2P and Cu-0.4P is 0.24, 0.56 and 1.22 wt.%, respectively, which is close to the theoretical value.

To confirm the effect of phosphorus addition on the microporous zeolitic structure before and after phosphorus introduction, hydrothermal aging and sulfur poisoning, N_2 sorption measurements, XRD and ^{27}Al MAS NMR were performed. As listed in Table 1, the low phosphorus loading does not significantly shrink the BET specific surface area and pore volume of the Cu-SSZ-13 catalyst. While the BET specific surface area reduces obviously from 622 cm^2/g to 561 cm^2/g as the phosphorus loading increases to 0.4 $mmol/g_{catal}$, implying that the effect of pore blocking by the deposition of phosphorus species cannot be ignored. After hydrothermal aging at 750℃ for 12 h, the BET specific surface area and pore volume of the fresh and phosphorus-impregnated Cu-SSZ-13 catalysts decrease markedly compared to the fresh counterparts as shown in Table S1 (in the Supporting information). In particular, the BET specific surface area and pore volume of the sulfurized samples (no regeneration) are decreased more severely, which may be ascribed to the blocking effect by the accumulation of sulfur species on the catalyst [32]. This result is in accord with previous investigations [19,32], which showed that the specific surface area and pore volume of Cu-SSZ-13 are decreased by hydrothermal treatment or the sulfur poisoning process.

As shown in Fig. 1a, all samples have the same CHA structure as confirmed by XRD analysis and no significant changes are observed in the diffraction peaks after 0.1 and 0.2 $mmol/g_{catal}$ phosphorous impregnation, suggesting that the crystalline structure is not influenced by a low-moderate content of introduced phosphorous. With further increase of the phosphorous loading (0.4 $mmol/g_{catal}$), an evident decrease of crystallinity is observed, indicating a deterioration of zeolitic frameworks. This result is further proved by the reduction in the BET specific surface area and pore volume after phosphorous impregnation. Upon hydrothermal treatment, a more severe decrease of crystallinity and a new amorphous silicon phase is visible (marked with ♥) [20,33] up to a high phosphorous loading (0.4 $mmol/g_{catal}$), revealing a local collapse of the framework structure, as shown in Fig. 1b. Compared with the XRD patterns of samples before and after aging, it can be asserted that the over-loading phosphorous addition accelerates the destruction of CHA structure during hydrothermal treatment. Upon sulfur poisoning, the variation trend of crystallinity is similar to that of the samples before sulfur poisoning (Fig. 1c). It indicates that the hydrothermal aging treatment has a more deteriorative effect on zeolitic structure than sulfur poisoning process as shown in Fig. S2. It is rational that the sulfur poisoning primarily acted as physical deposition and is detrimental to Cu species [34], which will be discussed in more detail below. Combined with XRD data, it is reasonable to assume that the

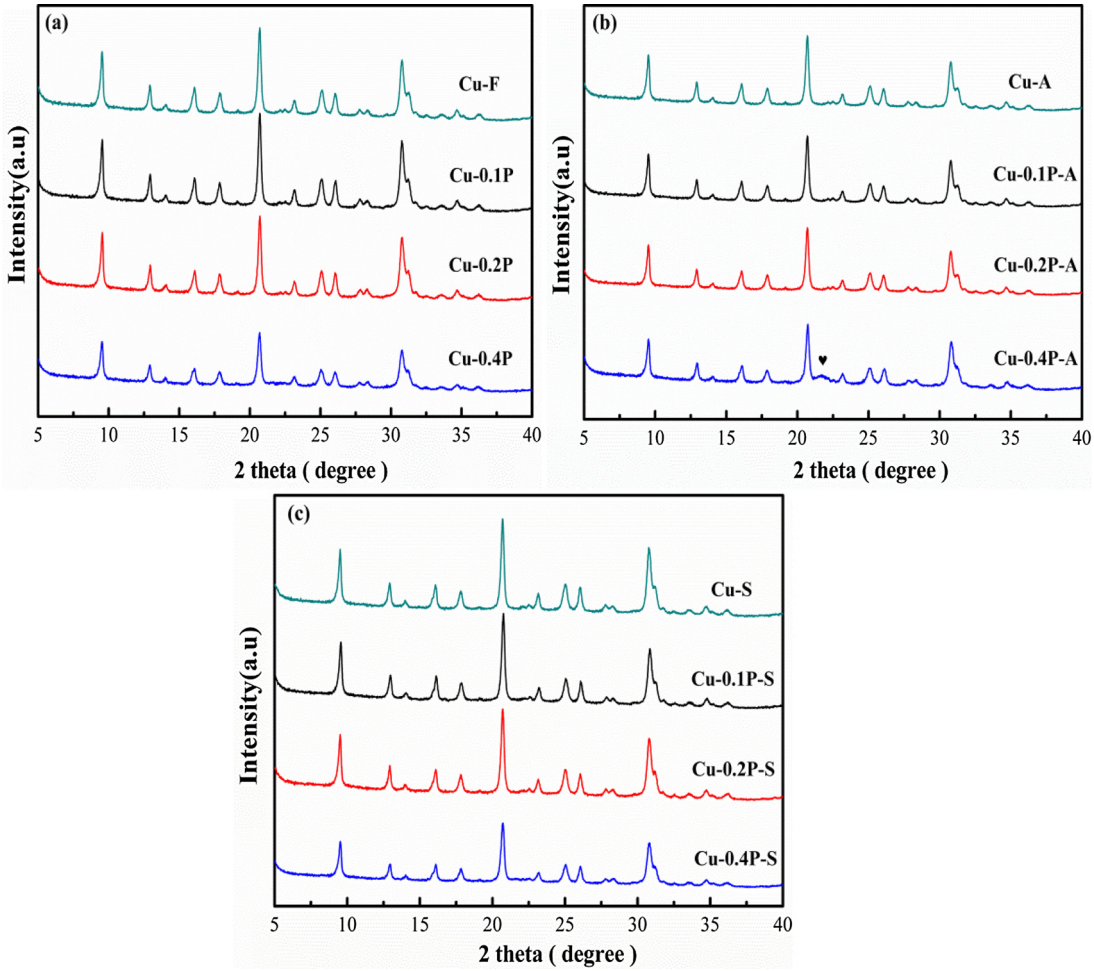

Fig. 1. XRD patterns of the fresh and phosphorous-impregnated Cu-SSZ-13 catalysts (a) as well as aged (b) and sulfur poisoned samples (c).

obvious decrease of BET specific surface area and pore volume are primarily caused by the accumulation of sulfur species [32].

To further examine framework dealumination of Cu-SSZ-13 after phosphorous impregnation, ^{27}Al MAS NMR spectra of the fresh, phosphorous-impregnated, hydrothermal aged and sulfurized samples were measured. The ^{27}Al MAS NMR spectra, as depicted in Fig. 2a, are dominated by a very intense peak at 58.5 ppm, attributed to tetrahedral Al species in the zeolitic framework [11,35]. Clearly, in agreement with the XRD data, the ^{27}Al MAS NMR profiles of Cu-F, Cu-0.1P and Cu-0.2P are almost identical, indicating that the low-moderate content of phosphorous addition has little effect on framework stability. Nevertheless, a new band was detected at approximately 40 ppm for Cu-0.4P. This band is related to the extraframework pentacoordinated Al sites [36,37], which can be corresponded to the dealumination of the sample [11,38], e.g., extra-framework aluminium phosphate or $CuAlO_2$. After hydrothermal treatment, the dealumination phenomenon is more evident for Cu-0.4P-A (Fig. 2b). Again, the spectra of aged Cu-SSZ-13 catalysts with low-moderate phosphorous content have not changed. It implies that the hydrothermal stability of Cu-SSZ-13 is deteriorated by introducing a relatively high concentration of phosphorous, which well agrees with the reduced crystallinity of the aged samples verified by XRD. No further significant framework dealumination could be detected upon sulfur poisoning as shown in Fig. 2c, which is in agreement with the XRD result and consistent with the viewpoint of Shen et al. [34] that SO_2 poisoning has a less pronounced effect on Cu-CHA framework structure. It illustrates that sulfur poisoning treatment does not further damage the framework structure of Cu-SSZ-13 with various phosphorus loadings.

Overall, combining the XRD analysis and ^{27}Al MAS NMR results, it is reasonable to speculate that the introduction of phosphorous promotes the dealumination process especially during hydrothermal aging, and these easily removable Al atoms may lead to a reduction in acid sites and active Cu species.

3.1.2. Changes of acidity

Fig. 3 shows NH_3-TPD results of the fresh, phosphorous-impregnated, aged and sulfur poisoned samples. Three NH_3 desorption peaks are observed for all samples. As believed by Epling [14,39] and other workers [40–42], the NH_3 desorption peak A–C at 150–180℃, 200–350℃ and 350–450℃ is corresponded to the weak acid sites resulting from surface hydroxyls and structural defects, strong Lewis acid sites stemming from exchanged Cu ions and Brønsted acid sites created by structural silicon hydroxyl groups, respectively. Interestingly, a decrease in Brønsted acid sites with increasing phosphorus loading is also noticed, as the peak at 430℃ decreases in intensity. Moreover, a shift to lower temperatures with increasing phosphorus loading is also observed, suggesting weaker Brønsted acid sites. Fig. 3d presents the amounts of NH_3 stored on the surface for all samples. It can be seen that the total amounts of NH_3 decrease with increasing phosphorus loading, indicating that the phosphorus poisoning suppresses the ammonia chemisorption at acid sites on Cu-SSZ-13 to some extent. These results are consistent with the studies reported by Olsson et al. [1,26], where increasing the phosphorus loading on Cu-SSZ-13 or Cu/BEA catalyst resulted in a decrease of NH_3 storage. In light of these findings, it can be concluded that the introduction of phosphorus not only decreases acid strength but also reduces acid amounts of Cu-SSZ-13 catalyst. This

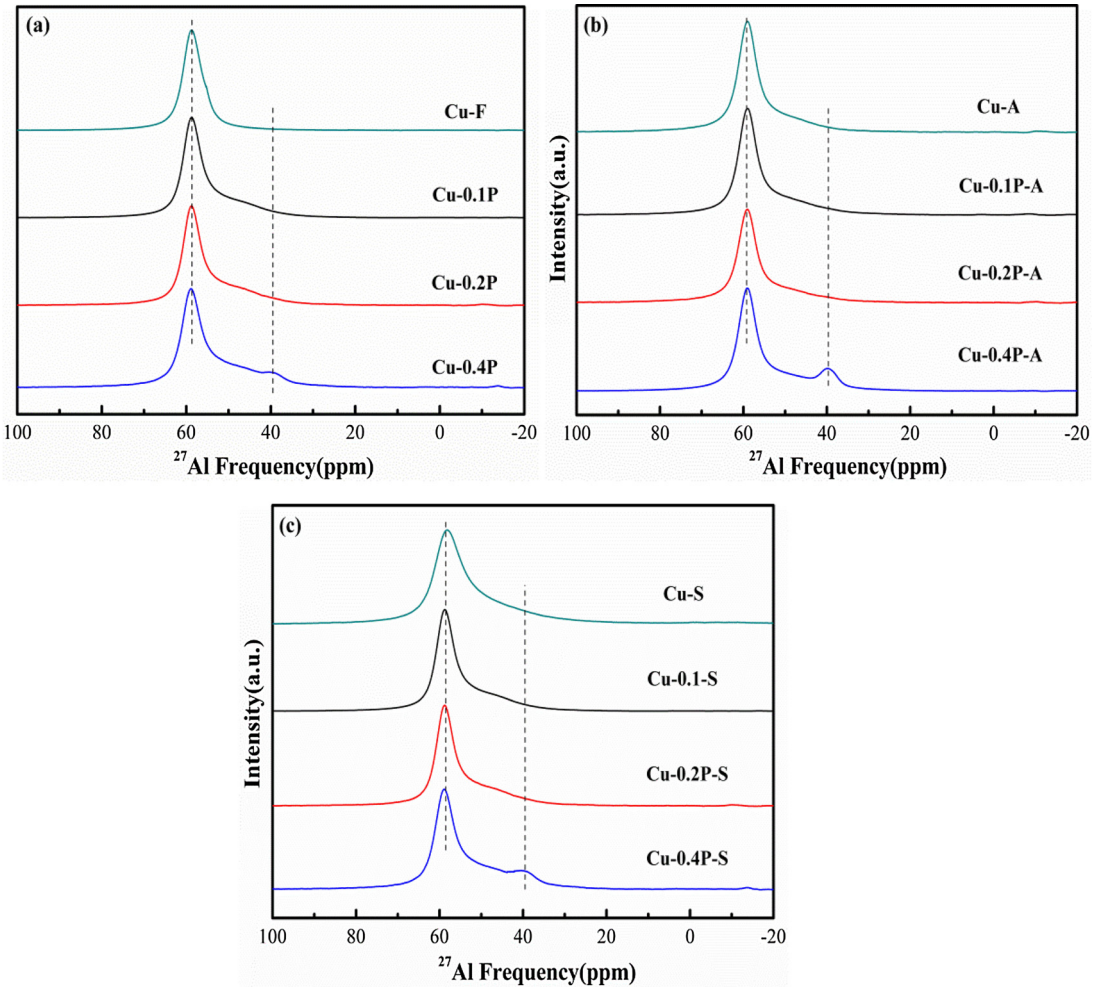

Fig. 2. ^{27}Al MAS NMR spectra of the fresh and phosphorous-impregnated Cu-SSZ-13 catalysts (a) as well as aged (b) and sulfur poisoned samples (c).

result is primarily due to the following reasons: (1) a portion of Brønsted acid sites are replaced by phosphorus species; (2) the local damages of zeolitic structure caused by framework dealumination upon phosphorus impregnation lead to a decrease in acid content and strength; (3) some acid sites tend to lose effectiveness owing to pore blocking by phosphate or metaphosphate [11,25]. Upon hydrothermal aging, although the decrease of acidity in phosphorus-impregnated samples remains, the differences among Cu-A and Cu-0.1P-A, Cu-0.2P-A and Cu-0.4P-A are insignificant. It suggests that the presence of phosphorus shows less influence on the acidity of aged samples. The acid strength of aged samples is also reduced with increasing phosphorus content. The NH_3-TPD measurements for sulfur poisoned samples before and after phosphorus impregnation were also performed. As shown in Fig. 3c, sulfur poisoning also leads to a further decrease in the number and strength of acid sites of impregnated samples compared to Cu-F. Compared with aged and sulfur poisoned samples, it is worth noting that the hydrothermal treatment has a more significant impact on acidity than the sulfur poisoning process, as shown in Fig. S4. It is most likely due to the hydrothermal aging treatment causing more destructive damage to the zeolitic structure than the sulfur poisoning treatment, as proved by XRD and ^{27}Al MAS NMR.

3.1.3. Evolution of Cu species

Fig. 4a represents the H_2-TPR profiles of the fresh and phosphorus-impregnated catalysts. As it can be seen, they reveal diverse reduction behaviors, clearly illustrating that the phosphorus impregnation has a significant influence on the distribution of Cu species in Cu-SSZ-13. For example, five peaks (A–E) centered at approximately 230℃, 300℃, 425℃, 650℃ and 865℃ appear on the Cu-F. According to previous reports [19,29,41,43,44], peaks A and C stand for the reduction of isolated Cu^{2+} ions at CHA cages and double six-rings (D6Rs) to Cu^+, respectively. Peak B could be assigned to the one-step reduction of CuO to Cu°. Peaks D and E indicate the reduction of two different types of Cu^+ into Cu°, which could be named "L(Low)-Cu^+" and "H(High)-Cu^+", respectively. After introducing phosphorus, a new copper species emerged that may be corresponded to the production of $CuAlO_2$ originating from the reaction between Cu^{2+} and $Al(OH)_3$ species from framework dealumination [38,45]. Obviously, the intensity of the $CuAlO_2$ peak increases with increasing phosphorus content, which is in accord with the result of ^{27}Al MAS NMR. Meanwhile, the intensity of peak A decreases and that of peak C increases after phosphorus impregnation, suggesting that some of the isolated Cu^{2+} ions migrate from CHA cage towards D6Rs. Importantly, after 0.1 $mmol/g_{catal}$ phosphorous impregnation, the amount of copper oxides is reduced. Olsson et al. [26] proposed that phosphorus interacts with oligomeric Cu_xO_y species inside the CHA cages, leading to the decrease of copper oxides content. Subsequently, the copper oxides increase with phosphorous content, which is in good agreement with the UV–vis-DRS results, as shown in Fig. S1 (The detailed explanations are also given in the Supporting information). It may be due to the destruction of the zeolitic framework, resulting in aggregation of copper species. Upon hydrothermal treatment, as shown in Fig. 4b, the copper species and the reducibility are similar between Cu-A and phosphorous-impregnated samples. It is probably due to the decomposition of phosphate species

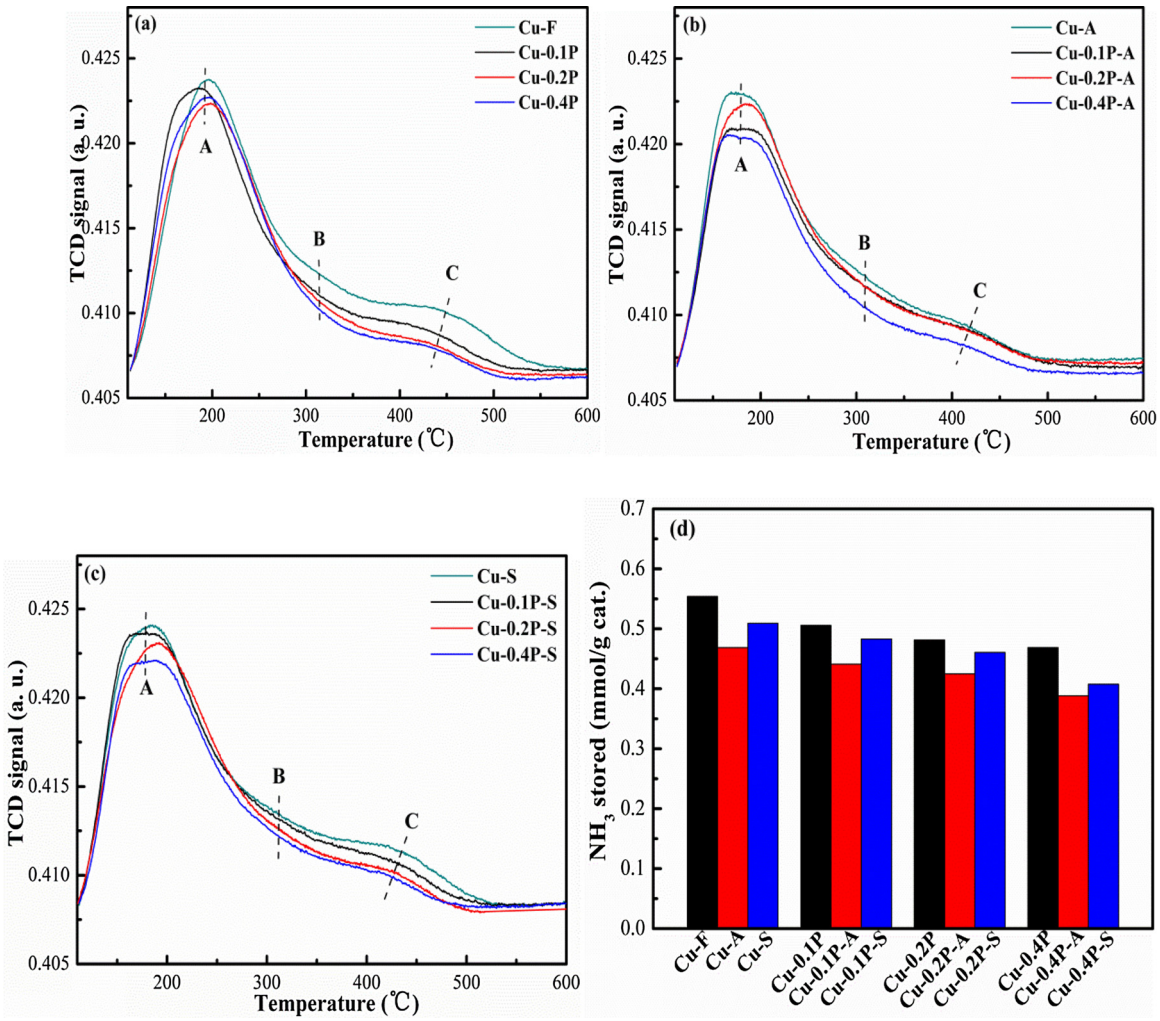

Fig. 3. NH_3-TPD profiles of the fresh and phosphorous-impregnated Cu-SSZ-13 catalysts (a) as well as aged (b) and sulfur poisoned samples (c). The amounts of NH_3 stored on the surface for these samples (d).

during high temperature hydrothermal aging. Fig. 4c presents the H_2-TPR profiles of sulfurized samples with different phosphorous loadings. Unexpectedly, even after regeneration (calcined at 550℃ for 2 h), it exhibits distinct reducibilities compared to the unvulcanized samples, meaning that the Cu state is changed remarkably after sulfurization. It is apparent that most isolated Cu^{2+} ions are no longer present in CHA cages, especially for phosphorous-impregnated samples. Meanwhile, the amount of isolated Cu^{2+} ions in D6Rs is increased after sulfurization. It indicates that some Cu^{2+} ions may migrate toward more stable locations and some other is formed copper sulfate. Certainly, the copper oxides are also reduced probably due to the interaction of copper oxides with sulfur to form copper sulfate, which is also examined using UV–vis-DRS. The formation of phosphate and sulfate can lead to pore blocking as confirmed by the severe decrease of specific surface area and pore volume. Hence, a portion of Cu sites can remain unavailable for reduction [1,46]. In light of the above observations, it can be reasonably concluded that the phosphorous addition, hydrothermal treatment and sulfur poisoning process results in significant changes in the redox properties of Cu-SSZ-13.

There tends to be a general agreement that the isolated Cu^{2+} ions are active sites in the NH_3-SCR reaction [47–49]. Consequently, to show directly the influence of phosphorus addition on the state of isolated Cu^{2+} ions, EPR analysis was used to quantify isolated Cu^{2+} ions in Cu-SSZ-13 samples. Fig. 5 shows the EPR spectra of the fresh, phosphorus-impregnated, hydrothermal aged and sulfur poisoned samples. It is observed that two major isolated Cu^{2+} ions, peak A ($g_{//}$ = 2.43 mT) and B ($g_{//}$ = 2.39 mT) assigned to isolated Cu^{2+} ions in D6Rs and CHA cages, respectively [50,51], are presented in all samples. After the introduction of phosphorus, the number of isolated Cu^{2+} ions decreases with the increase of phosphorus loading according to the semi-quantitative results by double integration of the EPR spectroscopy as summarized in Fig. 5d, which is also confirmed obtained by UV–vis-DRS as shown in Fig. S1. Beale et al. [11] also found by UV–vis-NIR DRS and XAS techniques that the number of isolated Cu^{2+} ions dramatically decreased and new Cu species are formed after introducing a large amount of phosphorus into Cu-SSZ-13 catalyst. Meanwhile, it is found that the decrease in the amount of isolated Cu^{2+} ions amount in our work is not as severe as that reported by Beale et al. It may be due to the higher phosphorus loading achieved by Beale et al. (2.2–8.8 wt.%) compared to our work (0.24–1.22 wt.%). Such a large number of phosphorus additions could result in a more serious destruction of the zeolitic structure and isolated Cu^{2+} ions. After hydrothermal treatment at 750℃, the aged samples show the same Cu^{2+} ion hyperfine features as the fresh counterparts and the number of isolated Cu^{2+} ions decreases, as depicted in Fig. 5b. However, the differences in the number of isolated Cu^{2+} ions between fresh and phosphorus-impregnated samples are negligible after aging, indicating that phosphorus has a minor effect on the stability of isolated Cu^{2+} ions during hydrothermal aging. Notably, the decrease in the amount of isolated Cu^{2+} ions for Cu-F (decreased by 20.7%) is more obvious than that of phosphorus-impregnated samples (decreased by 12.6%, 8.3% and 4.4% for Cu-0.1P, Cu-0.2P and Cu-0.4P, respectively). Upon sulfur poisoning, a

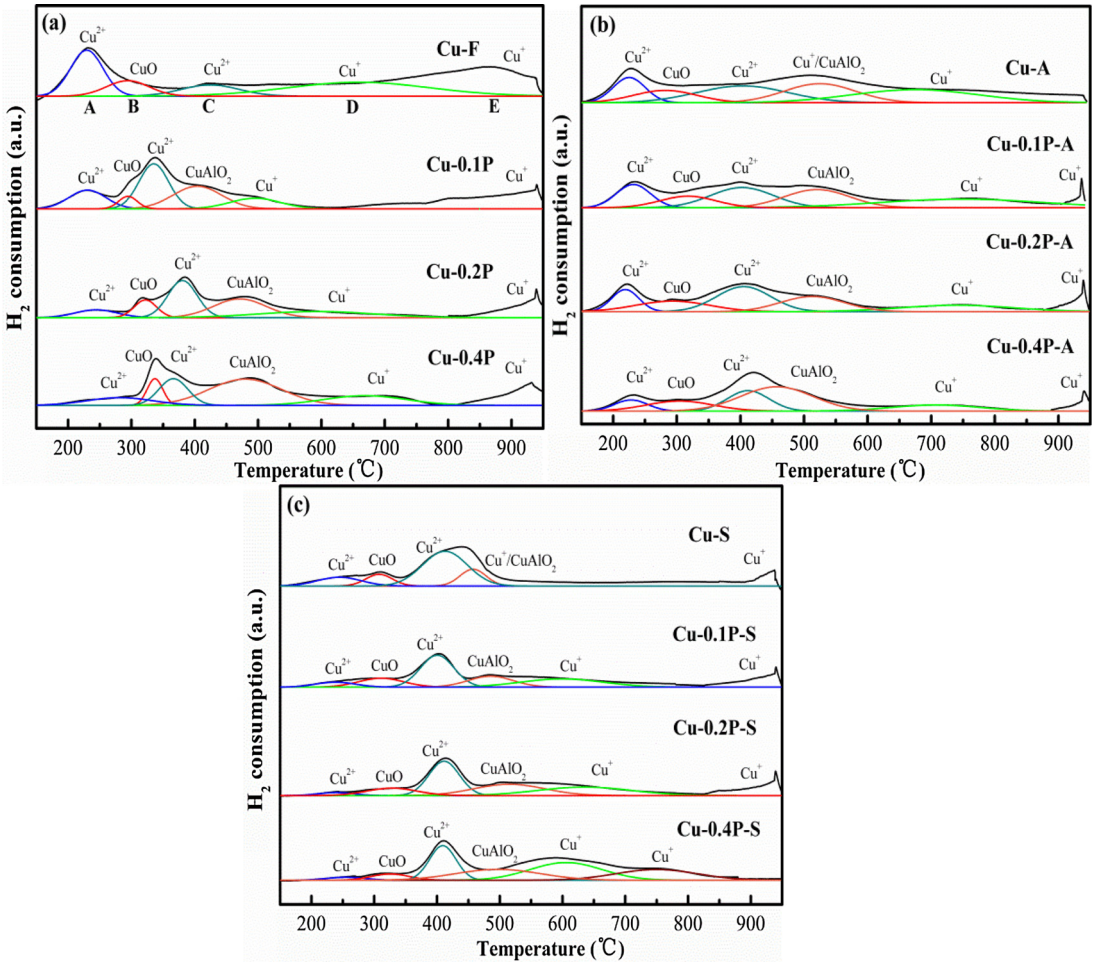

Fig. 4. H_2-TPR profiles of the fresh and phosphorous-impregnated Cu-SSZ-13 catalysts (a) as well as aged (b) and sulfur poisoned samples (c).

pronounced decrease in the number of isolated Cu^{2+} ions is found, as described in Fig. 5c and d. Compared with the fresh Cu-SSZ-13, the number of isolated Cu^{2+} ions for Cu-S, Cu-0.1P-S, Cu-0.2P-S and Cu-0.4P-S decreases by 48%, 49%, 52% and 57%, respectively. Epling et al. [52] discovered that the Z2Cu and ZCuOH sites are susceptible to severe low-temperature SO_2 poisoning because of the formation of highly stable bisulfite and ultimately bisulfate species. Therefore, the severe decrease in the number of isolated Cu^{2+} ions may be due to the interaction between isolated Cu^{2+} ions and sulfur species. Furthermore, the number of isolated Cu^{2+} ions decreases with increasing phosphorus loading, implying that phosphorus accelerates deactivation of Cu-SSZ-13 in the presence of SO_2.

A series of additional panels are also conducted to highlight the discrepancies between each treatment to Cu-SSZ-13, as described in Figs. S2–S7. An exhaustive discussion is provided in the Supporting information. In summary, as shown in Fig. 6, the deactivation mechanisms of Cu-SSZ-13 catalyst after phosphorus impregnation can be summarized as follows. After the introduction of phosphorus, a partial pore blocking and zeolitic framework dealumination occur, which leads to a reduction of acidity. Meanwhile, the interaction between phosphorus and copper species results in a decrease of copper oxides and isolated Cu^{2+} ions. Upon hydrothermal aging or sulfur poisoning, a further decrease in the specific surface area, acid sites and isolated Cu^{2+} ions is observed. In particular, phosphorus accelerates the zeolitic framework dealumination during hydrothermal aging and the reduction in the number of isolated Cu^{2+} ions after SO_2 poisoning.

3.2. Effect of phosphorus on the catalytic activity and durability of Cu-SSZ-13

Fig. 7a shows the catalytic activities of the fresh and phosphorus-impregnated samples. Interestingly, after the introduction of 0.1 mmol/g_{catal} phosphorus, the NO conversion of Cu-0.1P is enhanced evidently above 450℃,suggesting an inhibition effect of phosphorus on the NH_3 oxidation at high temperatures, which can be explained by the obvious decrease in the amount of CuO in Cu-0.1 P. With an increase in the phosphorus loading to 0.2 mmol/g_{catal}, the NO conversion of Cu-0.2P is also improved slightly above 525℃. Although phosphorus results in a slight decline in the NO conversion below 500℃, the deNO_x activity of Cu-0.2P remains largely intact over the entire temperature range. As expected, the deactivation effect of phosphorus on the catalytic activity is more pronounced after introducing 0.4 mmol/g_{catal} phosphorus into Cu-SSZ-13 catalyst. These seemingly strange results can be explained with the following facts. At low phosphorus loading, the copper oxides in the CHA cages could interact with phosphates to form copper phosphate species [26]. Hence, the amount of copper oxide could be reduced after introducing a low content of phosphorus, which is confirmed by H_2-TPR and UV–vis-DRS. There appears to be a general agreement that copper oxide is recognized as active site in the NH_3 oxidation reaction, which promotes NH_3 oxidation and accelerates NO_x generation at high temperatures. Thus, the enhancement of NO conversion at high temperatures for Cu-0.1P is largely attributed to the decrease of copper oxides. A similar phenomenon was also noticed by Olsson et al. [26] and ascribed to the severely suppressed NH_3 and NO oxidation reaction after phosphorus addition. Nevertheless, this

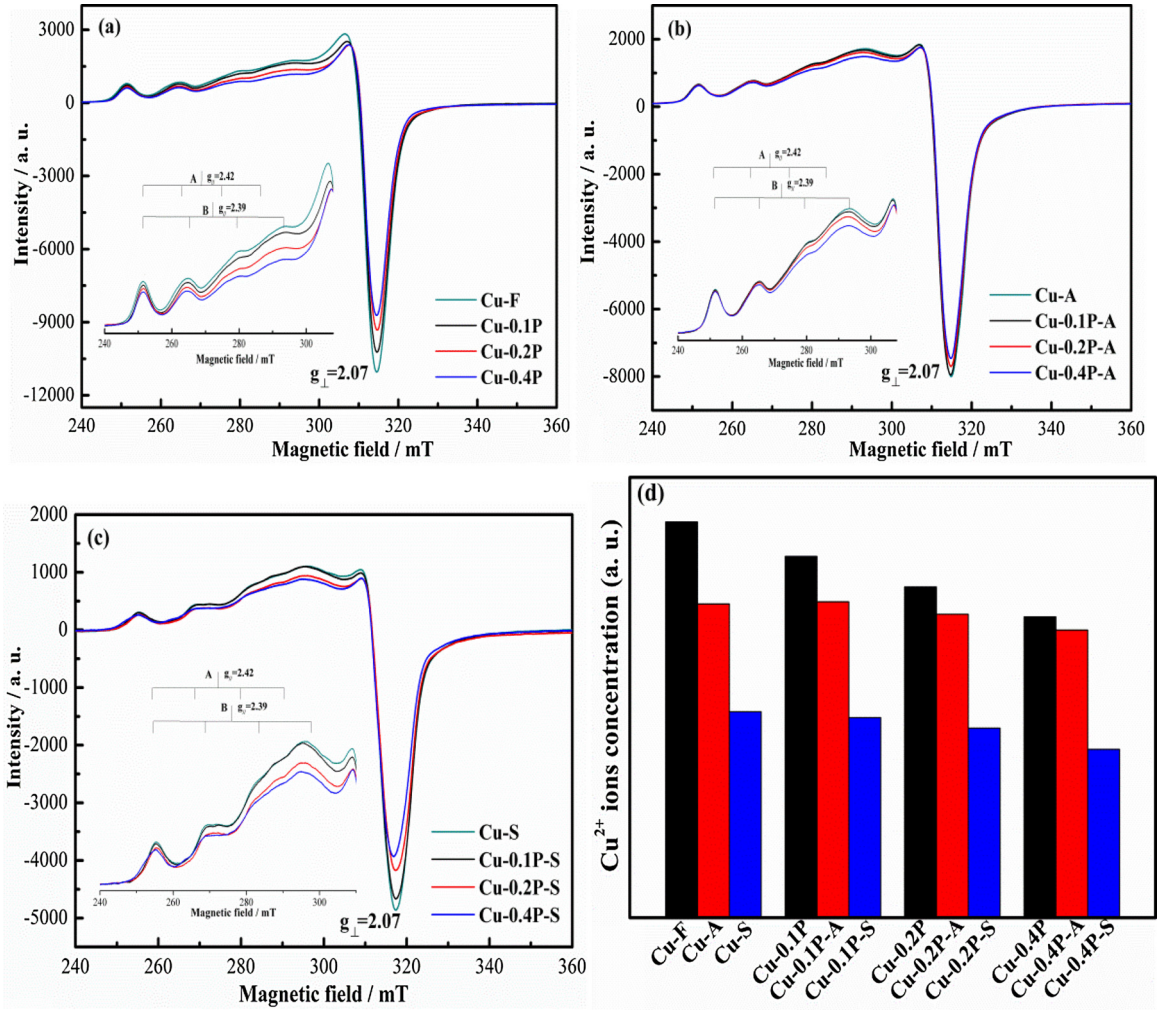

Fig. 5. EPR spectra of the fresh and phosphorous-impregnated Cu-SSZ-13 catalysts (a) as well as aged (b) and sulfur poisoned samples (c). The semi-quantitative amounts of isolated Cu^{2+} ions in these samples (d).

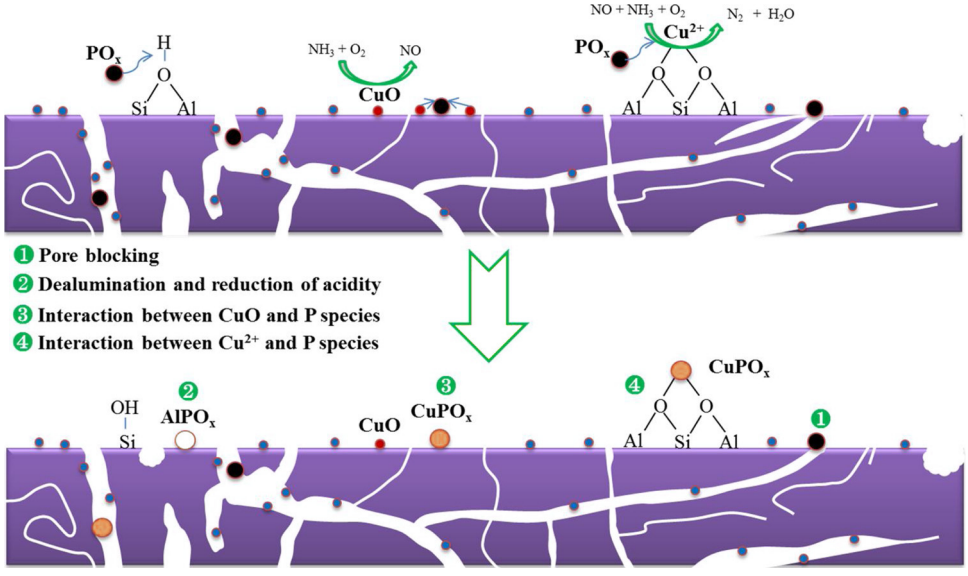

Fig. 6. Deactivation mechanism of Cu-SSZ-13 catalyst by phosphorus impregnation.

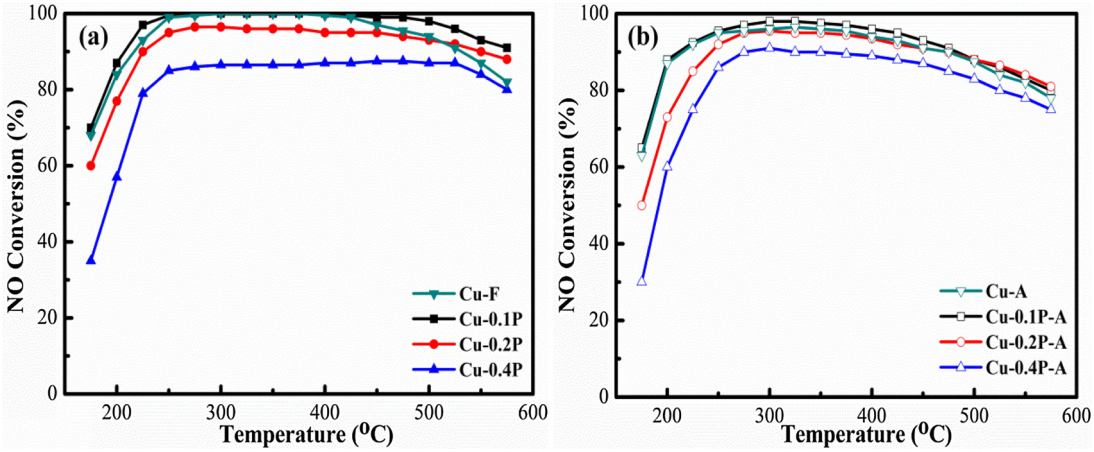

Fig. 7. NH_3-SCR performances of the fresh and phosphorus-impregnated Cu-SSZ-13 catalysts before (a) and after hydrothermal aging (b).

improved effect could also be observed after 0.4 mmol/g_{catal} of phosphorus introduction, in contrast to our results. This is probably a result of the discrepancies of Si/Al and Cu loading in the fresh Cu-SSZ-13 catalysts. The fresh Cu-SSZ-13 catalyst used by Olsson et al. has a lower Si/Al ratio (~6) and a higher Cu loading (~4.2 wt.%) compared with the Cu-F (Si/Al ratio = 15, Cu loading ~2.3 wt.%) in our work. As is well known, the lower Si/Al ratio leads to generation of more acid sites and exchange positions in Cu-SSZ-13. Therefore, the decrease in acid sites and isolated Cu^{2+} ions after phosphorus impregnation may have little effect on SCR performance. On the other hand, more copper oxides could be formed due to the high Cu loading in the Cu-SSZ-13 catalyst, resulting in a weak NO conversion at high temperatures. Hence, the content of copper oxides decreases dramatically even at a relatively high phosphorus impregnation level, which certainly contributes to an improvement of NO conversion at high temperatures. However, according to our previous work [20] and parameters of commercial Cu-SSZ-13 catalyst [15,53], the Cu-SSZ-13 with Si/Al = 15 and ~2.8 wt% Cu loading exhibits much better catalytic activity and hydrothermal stability than Cu-SSZ-13 with other Si/Al ratios. Therefore, in this work, the Cu-SSZ-13 with Si/Al = 15 and ~2.3 wt.% Cu loading is used to investigate the effect of phosphorus on SCR performance. After high phosphorus impregnation, a partial disruption and dealumination of zeolitic framework are observed together with aggregations of copper oxides, as verified by N_2 sorption, ^{27}Al MAS NMR and H_2-TPR. Simultaneously, the number of acid sites and isolated Cu^{2+} ions decrease evidently as proved by NH_3-TPD and EPR, respectively, which lead to the reduction in the NO conversion. Although the NO conversion decreases by 5–30% after introducing 0.4 mmol/g_{catal} phosphorus in our work, a complete suppression of the catalytic activity over the phosphorus-impregnated Cu-SSZ-13 catalyst was observed by Beale and et al. [11]. This distinction may contribute to the much higher phosphorus loading (> 2.2 wt.%) compared to our work (1.21 wt.%), leading to a stronger deactivation of the Cu-SSZ-13 catalyst [26].

Upon hydrothermal aging at 750°C for 12 h, the NO conversions over aged samples are decreased at low temperature range (< 250°C) and high temperature range (> 450°C), as described in Fig. 7b, probably due to the reduction of isolated Cu^{2+} ions, the increase of copper oxides and local damage of zeolitic structure. Cu-0.1 P-A and Cu-A exhibits a nearly identical performance to, meaning that Cu-SSZ-13 catalyst is resistant to the phosphorus poisoning at low phosphorus impregnation (≤0.1 mmol/g_{catal}). Compared with the Cu-A, Cu-0.2P-A shows nearly identical activities at high/moderate temperatures and lower activities at low temperatures. With a further increase in phosphorus loading to 0.4 mmol/g_{catal}, the deNO_x activities of Cu-0.4P-A decrease obviously over the entire temperature range, especially at low temperatures. For example, 87%, 88%, 73% and 60% NO conversions were obtained at 200°C over the Cu-A, Cu-0.1P-A, Cu-0.2P-A and Cu-0.4P-A, respectively. The above results indicate that the durability of Cu-SSZ-13 catalyst is not affected by the low content of phosphorus addition. When the impregnated content of phosphorus exceeds 0.2 mmol/g_{catal}, the durability of Cu-SSZ-13 catalyst begins to decrease. These results could be well explained by the changes in zeolitic structure, acidity and copper species on Cu-SSZ-13 after phosphorus impregnation.

3.3. Effect of phosphorus on the sulfur poisoning resistance of Cu-SSZ-13

To evaluate the effect of phosphorus on the sulfur poisoning resistance of Cu-SSZ-13 catalyst, the catalytic activities of monolith-supported fresh and phosphorus-impregnated catalysts were measured with a feed containing 1000 ppm NO, 1100 ppm NH_3, 25 ppm SO_2, 5% O_2, 10% H_2O, balance N_2 and with GHSV = 30,000 h^{-1}. The measurement for each sample was conducted for 120 min with a stepwise decrease in temperature 575–175°C. As presented in Fig. 8, the low temperature catalytic activity (175–350°C) of Cu-S significantly decreased compared to Cu-F (Fig. 6a), signifying that Cu-SSZ-13 catalyst is appreciably sensitive to sulfur poisoning at low temperatures. For example, the NO conversion decreased from 84% to 62% at 200°C. While there is no impact observed at high temperatures. This result is in accord with previous studies [32,54,55] proving that the effect of the sulfur poisoning was primarily apparent at low temperatures. After introducing phosphorus, the NO conversions are reduced remarkably

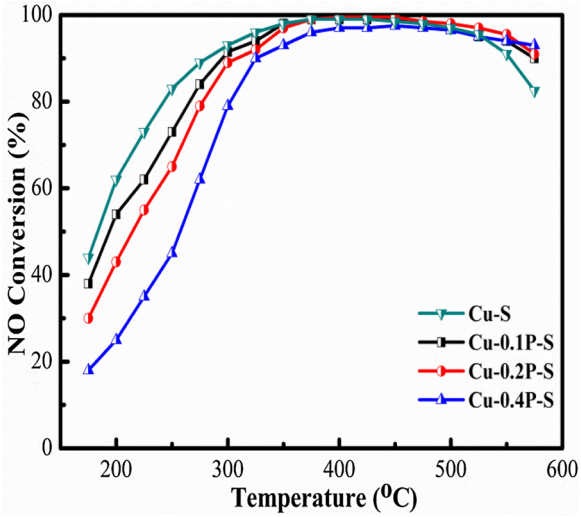

Fig. 8. NH_3-SCR performances of the fresh and phosphorus-impregnated Cu-SSZ-13 catalysts in the presence of SO_2.

with increasing phosphorus addition below 350℃. For example, 83%, 73%, 65% and 45% NO conversions were obtained at 250℃ over Cu-S, Cu-0.1P-S, Cu-0.2P-S and Cu-0.4P-S, respectively. It implies that the deactivation of Cu-SSZ-13 by SO_2 is much more severe after phosphorus impregnation. The declines of the acid sites and isolated Cu^{2+} ions are the powerful explanations for the decreased NO conversion of phosphorus-impregnated samples at low temperatures. Importantly, the number of acid sites decreases more after hydrothermal aging than after sulfur poisoning. Moreover, the crystallinity and integrity of the zeolitic framework of aged samples is lower than that of the sulfurized samples, as verified by XRD and ^{27}Al MAS NMR. However, the aged samples show much better catalytic activity than the sulfurized samples, so the reduction of acid sites is not solely responsible for catalyst deactivation. As confirmed by EPR, the number of isolated Cu^{2+} ions decreases by almost 45% after sulfur poisoning, which may be the main reason for the reduction in NO conversion at low temperatures. Additionally, Epling et al. [52] found that the low temperature activity of Cu-SSZ-13 catalyst was significantly inhibited by SO_2 due to the formation of ammonium sulfate and copper sulfate species by interacton of SO_2 with NH_3 and ZCuOH. A similar phenomenon is also observed over Cu-SAPO-34 catalyst [54,56]. As also confirmed by N_2 sorption in our work, the BET specific surface area for Cu-S, Cu-0.1P-S, Cu-0.2P-S and Cu-0.4P-S is reduced by 10.1%, 15.6%, 19.9% and 25.7%, respectively. However, the zeolitic structure is less affected by SO_2, as verified by XRD and ^{27}Al MAS NMR, suggesting the reduction of BET specific surface area due to the blocking effect. Accordingly, the sulfur accumulation and sulfate species formation (copper sulfate or ammonium sulfate species) on the surface of catalyst may also be important factors for the decrease of NO conversion. Notably, at high temperatures, the activities of the phosphorus-impregnated catalysts were slightly higher than that tested without SO_2, especially for Cu-0.4 P-S. It indicates that a promotive effect of SO_2 on the NO reduction over phosphorus-impregnated Cu-SSZ-13 occurs at high temperatures, which might be in response to the suppressed activity of NH_3 oxidation [32,54,56].

3.4. Effect of phosphorus on the NH3-SCR reaction kinetics of Cu-SSZ-13

To further understand the effect of phosphorus on the reaction kinetics of NO reduction over Cu-SSZ-13 catalysts, Arrhenius plots of the NH_3-SCR reaction under different conditions are shown in Fig. 9. All kinetic measurements were taken at < 20% NO conversion as depicted in Fig. S8. Fig. 9a shows Arrhenius plots of the reaction rate with respect to 1000/T over fresh Cu-SSZ-13 and impregnated catalysts with different phosphorus loadings. Adjacent to each plot, kinetic parameters including apparent activation energies (E_a) and pre-exponential factors (lnA) are displayed. It can be seen that Cu-F, Cu-0.1P and Cu-0.2P have similar E_a (~ 45 kJ/mol) and lnA (~3.9), indicating identical catalytic centers and rate-limiting steps [20,35]. It further demonstrates that the low-moderate phosphorus loading does not influence the NH_3-SCR mechanism over Cu-SSZ-13 catalyst [35]. Nevertheless, for Cu-0.4P, E_a and lnA values are considerably lower, indicating that the high content of phosphorus impregnation changes the NH_3-SCR reaction kinetic parameters over Cu-SSZ-13 catalyst, probably due to a change in the chemistry of the NH_3-SCR reaction [35,55]. It is also worth noting that the reaction rates appear to decrease as phosphorus addition increases, suggesting that phosphorus suppresses reaction rates. This result could be well explained by the damage to the zeolitic structure, the pore diffusion limitations, the formation of new Cu copper species and the reduction in the number of acid sites and isolated Cu^{2+} ions after the high concentration of phosphorus impregnation. After hydrothermal treatment, it is interesting that the discrepancies in E_a between Cu-0.4P and the other catalysts are negligible. The four almost parallel lines in Fig. 9b show that the aged catalysts have the same E_a, which verifies that the phosphorus does not affect the NH_3-SCR mechanism over Cu-SSZ-13 catalyst after hydrothermal treatment. This result can be attributed to the similar Cu species and considerable acidity. However, lnA decreases with increasing phosphorus addition after aging, which may be attributed to the reduction in the amount of isolated Cu^{2+} ions [34]. To further elucidate the effect of phosphorus on the resistance to sulfur poisoning, kinetic measurements in the presence of SO_2 were also performed over fresh and phosphorus-impregnated catalysts to obtain Arrhenius plots for comparison. As shown in Fig. 9c, Cu-S and Cu-0.1P-S have identical E_a and lnA. Simultaneously, E_a increases with the increase in phosphorus addition. Importantly, Cu-F, Cu-A and Cu-S exhibit strikingly similar E_a and lnA values (~ 45 kJ/mol and 3.1), indicating identical catalytic centers and rate-limiting steps after the hydrothermal treatment and sulfur poisoning over Cu-SSZ-13 catalyst [35]. Therefore, it can be further concluded that the high content of phosphorus alters the NH_3-SCR reaction kinetics parameters in the presence or absence of SO_2. It is probably due to damage to the zeolitic framework or the strong pore diffusion limitations after a high content of phosphorus is introduced, which leads to a change in the chemistry of the NH_3-SCR reaction [55]. Again, it is noticeable that reaction rates appear to decrease as phosphorus addition increases, suggesting that phosphorus reduces the sulfur poisoning resistance of Cu-SSZ-13 catalyst.

To summarize, in this work, we investigated systematically the effect of phosphorus on the physicochemical properties, catalytic activity, durability and sulfur poisoning resistance of Cu-SSZ-13 catalyst. The results show that the deleterious effect of phosphorus on Cu-SSZ-13 catalyst is larger than that of alkali and alkaline earth metals according to our previous report [19], where Cu-SSZ-13 could withstand the deactivation of a larger amount of (0.50 or 1.00 mmol/g_{catal}) alkali or alkaline earth metal impregnation under the same conditions. Simultaneously, Beale et al. [11] also found that phosphorus has a more significant deactivation than Pt, Zn or Ca on Cu-SSZ-13. In addition, the durability and sulfur poisoning resistance are reduced evidently at phosphorus content above 0.4 mmol/g_{catal}. Overall, the data herein presented provide a comprehensive picture of the interaction between phosphorus and the zeolitic framework, acid sites and copper species of Cu-SSZ-13, and especially clarify the variation of the NH_3-SCR reaction kinetic parameters after phosphorus addition. It certainly provides a significant theoretical basis for practical application of Cu-SSZ-13 or the design of novel catalysts to improve the performance of phosphorus resistance. Certainly, other issues such as the effect of phosphorus on fast NH_3-SCR reaction and N_2 selectivity over Cu-SSZ-13 also need to be further studied to provide more comprehensive information for application.

4. Conclusions

The influence of phosphorus on Cu-SSZ-13 catalyst for NH_3-SCR of NO is investigated by characterization and kinetic analysis. After a low content of phosphorus impregnation, a slight change in physicochemical properties (zeolitic framework, acidity and active Cu^{2+} ions) on Cu-SSZ-13 catalyst is found. However, it reduces the copper oxides, which leads to an enhancement of NO conversion at high temperatures. When the phosphorous loading exceeds 0.40 mmol/g_{catal}, it is found to inhibit the SCR activity of Cu-SSZ-13 over the entire temperature range, which is attributable to the obvious reduction in the acid sites and isolated Cu^{2+} ions. Moreover, the decrease of crystallinity caused by zeolitic framework dealumination after a high content of phosphorous introducing is also observed. Phosphorous accelerates the dealumination during hydrothermal aging, which results in a significant decrease in the durability of Cu-SSZ-13 catalyst with high phosphorus impregnation. The effect of phosphorous on the sulfur poisoning resistance of Cu-SSZ-13 is also studied. The NO conversions are decreased dramatically with increasing phosphorous loading in the presence of SO_2 below 350℃, suggesting that phosphorous reduces the sulfur poisoning resistance of Cu-SSZ-13. The kinetic analysis further proves that the low phosphorous loading does not affect the apparent activation energies and pre-exponential factors. Nevertheless, the apparent

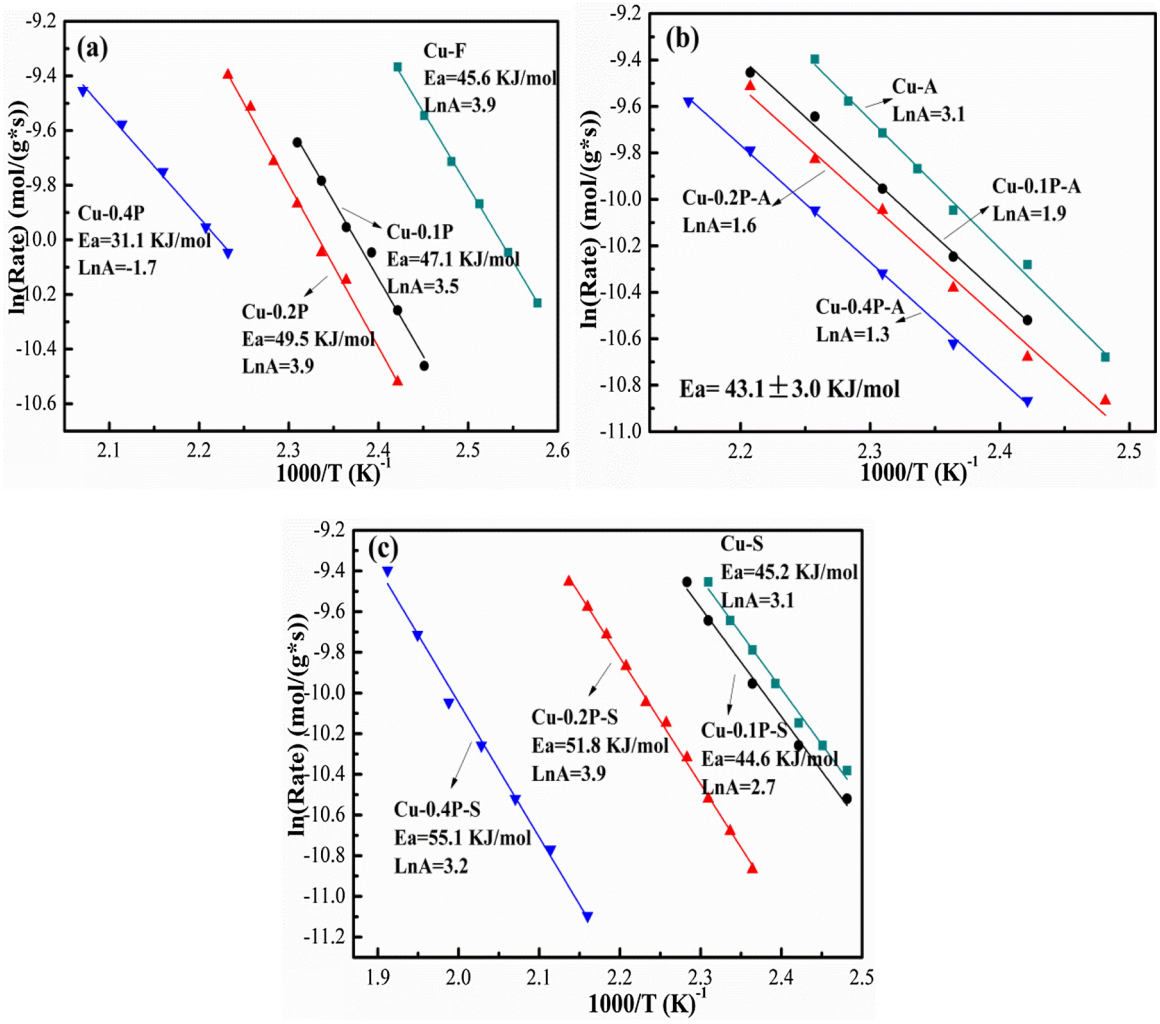

Fig. 9. $Rate_{NO}$ of NH_3-SCR reaction over fresh and phosphorus-impregnated Cu-SSZ-13 catalysts as a function of reaction temperature (a) as well as aged (b) and sulfur poisoned samples (c).

activation energies and pre-exponential factors are changed with increasing phosphorous addition. Compared to our previous findings, the Cu-SSZ-13 catalyst is more sensitive to deactivation by phosphorous than by alkali and alkaline earth metals.

Acknowledgements

The authors gratefully acknowledge financial support from the National Natural Science Foundation of China (21473064) and the Analytical and Testing Center of Huazhong University of Science and Technology for the use of its facilities.

Appendix A. Supplementary data

Supplementary material related to this article can be found, in the online version, at doi:https://doi.org/10.1016/j.apcatb.2018.05.075.

References

[1] S. Andonova, E. Vovk, J. Sjöblom, E. Ozensoy, L. Olsson, Appl. Catal. B: Environ. 147 (2014) 251–263.
[2] L. Pang, C. Fan, L. Shao, K. Song, J. Yi, X. Cai, J. Wang, M. Kang, T. Li, Chem. Eng. J. 253 (2014) 394–401.
[3] Y. Xin, Q. Li, Z. Zhang, ChemCatChem 10 (2018) 29–41.
[4] J.H. Kwak, R.G. Tonkyn, D.H. Kim, J. Szanyi, C.H.F. Peden, J. Catal. 275 (2010) 187–190.
[5] J. Luo, H. An, K. Kamasamudram, N. Currier, A. Yezerets, T. Watkins, L. Allard, SAE Int. J. Engines 8 (2015) 2015-01-1022.
[6] J. Wang, H. Zhao, G. Haller, Y. Li, Appl. Catal. B: Environ. 202 (2017) 346–354.
[7] S.Y. Joshi, A. Kumar, J. Luo, K. Kamasamudram, N.W. Currier, A. Yezerets, Appl. Catal. B: Environ. 226 (2018) 565–574.
[8] U. Deka, I. Lezcano-Gonzalez, B.M. Weckhuysen, A.M. Beale, ACS Catal. 3 (2013) 413–427.
[9] R. Zhang, J.-S. McEwen, M. Kollár, F. Gao, Y. Wang, J. Szanyi, C.H.F. Peden, ACS Catal. 4 (2014) 4093–4105.
[10] A.M. Beale, F. Gao, I. Lezcano-Gonzalez, C.H.F. Peden, J. Szanyi, Chem. Soc. Rev. 44 (2015) 7371–7405.
[11] I. Lezcano-Gonzalez, U. Deka, H.E. van der Bij, P. Paalanen, B. Arstad, B.M. Weckhuysen, A.M. Beale, Appl. Catal. B: Environ. 154–155 (2014) 339–349.
[12] Y.J. Kim, J.K. Lee, K.M. Min, S.B. Hong, I.-S. Nam, B.K. Cho, J. Catal. 311 (2014) 447–457.
[13] S. Shwan, J. Jansson, L. Olsson, M. Skoglundh, Appl. Catal. B: Environ. 147 (2014) 111–123.
[14] D. Wang, Y. Jangjou, Y. Liu, M.K. Sharma, J. Luo, J. Li, K. Kamasamudram, W.S. Epling, Appl. Catal. B: Environ. 165 (2015) 438–445.
[15] S.J. Schmieg, S.H. Oh, C.H. Kim, D.B. Brown, J.H. Lee, C.H.F. Peden, D.H. Kim, Catal. Today 184 (2012) 252–261.
[16] G. Cavataio, H.-W. Jen, D.A. Dobson, J.R. Warner, SAE Int. (2009) 2009-01-2823.
[17] W. Shan, H. Song, Catal. Sci. Technol. 5 (2015) 4280–4288.
[18] O. Kröcher, M. Elsener, Appl. Catal. B: Environ. 77 (2008) 215–227.
[19] C. Fan, Z. Chen, L. Pang, S. Ming, C. Dong, K. Brou Albert, P. Liu, J. Wang, D. Zhu, H. Chen, T. Li, Chem. Eng. J. 334 (2018) 344–354.
[20] C. Fan, Z. Chen, L. Pang, S. Ming, X. Zhang, K.B. Albert, P. Liu, H. Chen, T. Li, Appl. Catal. A: Gen. 550 (2018) 256–265.
[21] P. Wang, S. Chen, S. Gao, J. Zhang, H. Wang, Z. Wu, Appl. Catal. B: Environ. 231 (2018) 299–309.
[22] N.-Z. Yang, R.-T. Guo, Q.-S. Wang, W.-G. Pan, Q.-L. Chen, C.-Z. Lu, S.-X. Wang, RSC Adv. 6 (2016) 11226–11232.
[23] Y. You, H. Chang, T. Zhu, T. Zhang, X. Li, J. Li, Mol. Catal. 439 (2017) 15–24.
[24] R.G. Silver, M.O. Stefanick, B.I. Todd, Catal. Today 136 (2008) 28–33.

[25] H.E. van der Bij, B.M. Weckhuysen, Chem. Soc. Rev. 44 (2015) 7406–7428.
[26] K. Xie, K. Leistner, K. Wijayanti, A. Kumar, K. Kamasamudram, L. Olsson, Catal. Today 297 (2017) 46–52.
[27] U. Deka, A. Juhin, E.A. Eilertsen, H. Emerich, M.A. Green, S.T. Korhonen, B.M. Weckhuysen, A.M. Beale, J. Phys. Chem. C 116 (2012) 4809–4818.
[28] N. Martin, Z. Li, J. Martinez-Triguero, J. Yu, M. Moliner, A. Corma, Chem. Commun. 52 (2016) 6072–6075.
[29] F. Gao, E.D. Walter, E.M. Karp, J. Luo, R.G. Tonkyn, J.H. Kwak, J. Szanyi, C.H.F. Peden, J. Catal. 300 (2013) 20–29.
[30] F. Gao, Y. Wang, M. Kollár, N.M. Washton, J. Szanyi, C.H.F. Peden, Catal. Today 258 (2015) 347–358.
[31] P. Chavannavar, SAE Int. (2012) 2012-01-1299.
[32] K. Wijayanti, K. Leistner, S. Chand, A. Kumar, K. Kamasamudram, N.W. Currier, A. Yezerets, L. Olsson, Catal. Sci. Technol. 6 (2016) 2565–2579.
[33] R. Martínez-Franco, M. Moliner, P. Concepcion, J.R. Thogersen, A. Corma, J. Catal. 314 (2014) 73–82.
[34] M. Shen, H. Wen, T. Hao, T. Yu, D. Fan, J. Wang, W. Li, J. Wang, Catal. Sci. Technol. 5 (2015) 1741–1749.
[35] F. Gao, N.M. Washton, Y. Wang, M. Kollár, J. Szanyi, C.H.F. Peden, J. Catal. 331 (2015) 25–38.
[36] Q. Zhu, J.N. Kondo, R. Ohnuma, Y. Kubota, M. Yamaguchi, T. Tatsumi, Microporous Mesoporous Mater. 112 (2008) 153–161.
[37] J.H. Yun, R.F. Lobo, Catal. Sci. Technol. 5 (2015) 264–273.
[38] Z. Zhao, R. Yu, R. Zhao, C. Shi, H. Gies, F.-S. Xiao, D. De Vos, T. Yokoi, X. Bao, U. Kolb, M. Feyen, R. McGuire, S. Maurer, A. Moini, U. Müller, W. Zhang, Appl. Catal. B: Environ. 217 (2017) 421–428.
[39] D. Wang, F. Gao, C.H.F. Peden, J. Li, K. Kamasamudram, W.S. Epling, ChemCatChem 6 (2014) 1579–1583.
[40] I. Lezcano-Gonzalez, U. Deka, B. Arstad, A. Van Yperen-De Deyne, K. Hemelsoet, M. Waroquier, V. Van Speybroeck, B.M. Weckhuysen, A.M. Beale, PCCP 16 (2014) 1639–1650.
[41] T. Zhang, F. Qiu, J. Li, Appl. Catal. B: Environ. 195 (2016) 48–58.
[42] R. Oord, I.C. ten Have, J.M. Arends, F.C. Hendriks, J. Schmidt, I. Lezcano-Gonzalez, B.M. Weckhuysen, Catal. Sci. Technol. 7 (2017) 3851–3862.
[43] B. Chen, R. Xu, R. Zhang, N. Liu, Environ. Sci. Technol. 48 (2014) 13909–13916.
[44] M. Xu, J. Wang, T. Yu, J. Wang, M. Shen, Appl. Catal. B: Environ. 220 (2018) 161–170.
[45] W. Su, Z. Li, Y. Peng, J. Li, PCCP 17 (2015) 29142–29149.
[46] K. Wijayanti, S. Andonova, A. Kumar, J. Li, K. Kamasamudram, N.W. Currier, A. Yezerets, L. Olsson, Appl. Catal. B: Environ. 166–167 (2015) 568–579.
[47] L. Ma, Y. Cheng, G. Cavataio, R.W. McCabe, L. Fu, J. Li, Chem. Eng. J. 225 (2013) 323–330.
[48] J. Wang, D. Fan, T. Yu, J. Wang, T. Hao, X. Hu, M. Shen, W. Li, J. Catal. 322 (2015) 84–90.
[49] S. Han, Q. Ye, S. Cheng, T. Kang, H. Dai, Catal. Sci. Technol. 7 (2017) 703–717.
[50] A. Godiksen, F.N. Stappen, P.N.R. Vennestrøm, F. Giordanino, S.B. Rasmussen, L.F. Lundegaard, S. Mossin, J. Phys. Chem. C 118 (2014) 23126–23138.
[51] Y. Shan, X. Shi, Z. Yan, J. Liu, Y. Yu, H. He, Catal. Today (2017), http://dx.doi.org/10.1016/j.cattod.2017.11.006 in press.
[52] Y. Jangjou, Q. Do, Y. Gu, L.-G. Lim, H. Sun, D. Wang, A. Kumar, J. Li, L.C. Grabow, W. Epling, ACS Catal. 8 (2018) 1325–1337.
[53] S. Prodinger, M.A. Derewinski, Y. Wang, N.M. Washton, E.D. Walter, J. Szanyi, F. Gao, Y. Wang, C.H.F. Peden, Appl. Catal. B: Environ. 201 (2017) 461–469.
[54] L. Zhang, D. Wang, Y. Liu, K. Kamasamudram, J. Li, W. Epling, Appl. Catal. B: Environ. 156–157 (2014) 371–377.
[55] P.S. Hammershøi, Y. Jangjou, W.S. Epling, A.D. Jensen, T.V.W. Janssens, Appl. Catal. B: Environ. 226 (2018) 38–45.
[56] C. Wang, J. Wang, J. Wang, T. Yu, M. Shen, W. Wang, W. Li, Appl. Catal. B: Environ. 204 (2017) 239–249.